Circuits, Systems, and Signal Processing
https://doi.org/10.1007/s00034-025-03096-8

A Novel Ensemble Empirical Decomposition and Time–Frequency Analysis Approach for Vibroarthrographic Signal Processing

Surbhi Bhatia Khan[1,2,3] · A. Balajee[4] · S. Sheik Mohideen Shah[5] · T. R. Mahesh[4] · Mohammad Alojail[6] · Indrajeet Gupta[7]

Received: 27 August 2024 / Revised: 4 March 2025 / Accepted: 5 March 2025

Abstract

Signal processing techniques play a critical role in addressing real-world applications across domains such as sensor analysis, defence, and clinical and biomedical fields. Within healthcare, computer-aided diagnostic (CAD) systems have become pivotal in supporting medical professionals with the interpretation of data and images, especially in medical imaging and radiological diagnostics. For diagnosing joint disorders, both time-domain and frequency-domain analyses are employed to examine complex, non-stationary, and nonlinear signals. To process Vibroarthrographic signals in this context, an initial step involves applying the Hilbert-Huang Transform, which comprises two stages: Empirical Mode Decomposition (EMD) for computing intrinsic mode functions (IMFs), followed by the Hilbert transform for further signal analysis. In our proposed approach, we utilized Complete Ensemble Empirical Mode Decomposition with Adaptive Noise and Time-Varying Frequency Empirical Mode Decomposition (TVF-EMD) to compute IMFs, as well as Variation Mode Decomposition to calculate mode signals. Subsequent feature extraction incorporates both time and frequency characteristics, focusing on metrics such as pixel intensity, mean, and standard deviation. These features then serve as inputs to machine learning models for classification tasks, distinguishing between healthy and non-healthy signal samples. In our model, we employed a Least Squares Support Vector Machine (LS-SVM) and a Support Vector Machine with Recursive Feature Elimination (SVM-RFE) to enhance classification accuracy. This sequence of signal processing and machine learning steps demonstrates a structured and effective approach for CAD-based diagnosis in joint disorder assessments.

Keywords Vibroarthrography · Joint disorder · Empirical decomposition · Signal processing · Machine learning

Extended author information available on the last page of the article

Published online: 11 April 2025

1 Introduction

One of the critical disorder analyses in the medical field trending nowadays is the diagnosis of joint disorders, which are very complex due to the structure of the different human joints, namely, shoulder joints, hip joints, elbow joints, and knee joints. At present, there are two different methods of diagnosing in practice. One is the invasive method, and the second one is the non-invasive method. An invasive method is similar to arthroscopy, as it is not only expensive but not suitable for regular diagnostics [9]. The other disadvantage of this method is that it is entirely prone to infection [1]. An alternative diagnostic method is a non-invasive method; similar methods include computer tomography (CT), magnetic resonance imaging (MRI), X-rays, etc.

Vibroarthrography (VAG) method is one of the non-invasive methods. This follows the natural phenomena of performing analysis of high-frequency vibroacoustic radiation, which is obtained from the relative movement of articular surfaces of the synovial joint (diarthrosis) [20]. In physical conditions, articulate the outside is covered by hyaline ossein that is smooth and slimy, which detects optimal arthro-kinematic movement quality. Osteoarthritis is again and again observed by using the Patello Femoral Joint (PFJ) [8]. A portion of the knee joint is complex and can be explained by its specified biomechanical surroundings and massive involvement in day-to-day activity. VAG signals onward Computer Aided Diagnostic could contribute those attributes for diagnosing knee joint disorders. VAG signals work on the basis of acoustic sounds or the other vibrations sound emitted from the mid of the patella at the time of active movements at the leg. VAG signals exhibit the ability of non-linearity, multi-component and are non-stationary in nature [18]. Thus, the analysis of VAG signals would not be preferred for digital signal processing using conventional methods. The greatest awareness of the VAG test results from the skin-deep position of the knee. Commonly, the knee joint is analyzed using VAG Diagnostic [4].

The VAG method could be helpful in differentiating individual disorders of the Patello Femoral Joint (PFJ) and its stages, in that the unique, disorder-relevant attribute of the VAG signal pattern. Yet, at the time of the problem, the classification of normal and abnormal VAG signals has been prepared and extending it to a multiclass classification remainder essentially unaddressed [12]. Moreover, as previously suggested, further work is needed to determine in case the sensitivity and particularity of the VAG method are acceptable for analytic application. As well, there is an insistent need for an explanation of optimal algorithms for VAG signal multiclass classification according to the analytical criteria of PFJ chondral lesions [2]. Optimization of diagnostic methods must include the selection of the most relevant and discriminating VAG signal parameter values, further by the selection of an optimal predictive model. This will allow us to develop an observed independently, sensitive computer-aided diagnostic method, useful for analysers, mainly for orthopedists and physiotherapists, who are troubled with an evaluation of the quality of arthrokinematic movement as physical examination [28].

Thus, the Initial goal of this preparation for to extend the VAG signal arrangement of various PFJ chondral lesions to a 5-class classification (normally and four classes of disorders). Our analyses will be operated with respect to the MRI diagnosis as a reference method of non-invasive estimate of chondral lesions, that have allowed us to evaluate the positive rate and true negative rate of the VAG method [5]. For the optimization problem, two algorithms were used to select the best parameter value: genetic search and selection based on in-complex regression functions. Then, we compare four classification models representing various approaches to the classification problem: logistic regression with automatic attribute selection based on multilayer perceptron, in-complex regression functions, sigmoid stimulating function, sequential minimal optimization algorithm implementation of support vector machine classifier and random forest tree.

The VAG method is still in development; it displays high accuracy, sensitivity and specificity when comparing results achieved from controls and a non-specified knee-joint disorder group. In applied to the Least Square—Support Vector Machines (LS-SVM) algorithm established on the time complexity parameters of the VAG signal and achieved greater than 94% classification accuracy, greater than 98% sensitivity and 86% specificity. The classification of the neural network with frequency parameters as inputs has allowed for improvement of the accuracy to more than 95%, sensitivity of 92% and specificity of more than 98%. The best results of the normal and abnormal classification signals are found. A classifier based on a radial-based function network with statistical parameters in the time domain achieved accuracy, sensitivity, and specificity of 96%, with the cross-validation of the leave-one-out method [16].

Visualizing the knee joint as X-rays at the different time stamps also used ultrasound. Invasive methods are commonly performed via image review, and they could not provide information about the early bone disorder [28. On the other hand, early diagnosis of bone joint disorder using non-invasive methods had analysed the bone joint disorder surface using LabVIEW software with the help of acquired VAG Signal [17]. The state-of-art models used for comparison are given in the following Table 1.

Thus, through various studies on problem statements and by working with the existing methods, we framed the objectives that led to the following major contributions.

Table 1 Comparison of existing models

Study	Accuracy (%)	Observation
Yang et al. [29]	86	Dynamic Knee motions were recorded using CT bone models and the results are analyzed using KL Grades
Satheesh et al. [19]	91	Soft tissue contrast points were analyzed by reviewing numerous MRI images and the metrics comparison is done with different SVM models
RM Rangayyan and Y. Wu [18]	82	VAG signals are extracted using interior and exterior movement and the results are analyzed using LS-SVM
Wu Yungfeng [28]	89	Signal processing models are suggested for the extraction of VAG and the comparison of results are done using Random Forest algorithm
Rajalakshmi et al. [17]	93	The VAG signals acquired on the surface of the suspicious bone joint are analyzed using LabVIEW software which yields information regarding the bone disorders

- Construction of Intrinsic Mode Functions (IMF) from the raw VAG signal to analyse the time-series of the data.
- Complete Empirical Mode Decomposition and Time-Varying Frequency Empirical Mode Decomposition for calculating the non-linearity within the VAG signal
- Support Vector Machine integrated Recursive Feature Elimination model to obtain an optimal feature set.
- Classification of Healthy and Unhealthy signals using the Least Square Support Vector Machine.

In this paper, Sect. 1 explains the basic introduction to Vibroarthrographic (VAG) signal and its importance in finding healthy and unhealthy knee joint disorders. Section 2 briefly explains methodologies, including CEEMDAN, TVF-EMD, and VMD methods, as well as feature extraction algorithms like SVM, LS-SVM, and SVM-RFE. Section 3 majorly covers the results and discussion of executed methodologies, followed by a conclusion and references.

2 Methodologies

This section covers the major methodologies focussed on the process of analysing joint disorders using VAG signals. VMD, TVF-EMD and CEEMDAN are the three different methods of algorithm which are used to get the input from VAG signals like EEG, ECG, and EMG etc. Further processing on TVF-EMD signal noise-related data analysis that estimates the means of IMFs from the input data, combined with white noise, helps to remove noise using IMF's signals. The VAG signal is re-constructed by dominant IMF, and TFD (TFD-Time frequency domain) is achieved by using Hilbert transformation-(HT). Time–frequency distribution- (TFD) contains a time–frequency image, and statistical features consisting of mean and standard deviation are extracted from the time–frequency image [6]. This methodology is based on a non-stationary, nonlinear adaptive signal processing technique.

The VMD signal central frequency uses an estimate of each mode of bandwidth signal [27]. EMD was specifically developed for time–frequency analysis of nonlinear signals [15]. CEEMDAN is a deviation of the EEMD method that provides an exact reconstruction of the original signal. Then, it has a better spectral partition of the IMFs [32]. All the above signals are performed as Hilbert Huang Transformation (HHT) is a process to decompose a signal as intrinsic mode functions (IMFs) and gather instantaneous frequency data. To construct Intrinsic Mode Functions (IMFs) from raw vibroarthrographic (VAG) signals, a process like Complete Ensemble Empirical Mode Decomposition with Adaptive Noise (CEEMDAN) is often used, as it provides a robust framework to handle the inherent non-linear and non-stationary nature of VAG signals. The process begins by adding white noise to the raw VAG signal, which helps prevent mode mixing, a common issue where different frequency components overlap within the same IMF. The CEEMDAN algorithm iteratively decomposes the signal by applying an empirical mode decomposition (EMD) to extract each IMF sequentially. For each iteration, the first IMF is derived by identifying and extracting the highest frequency oscillatory mode present in the signal, following a sifting process

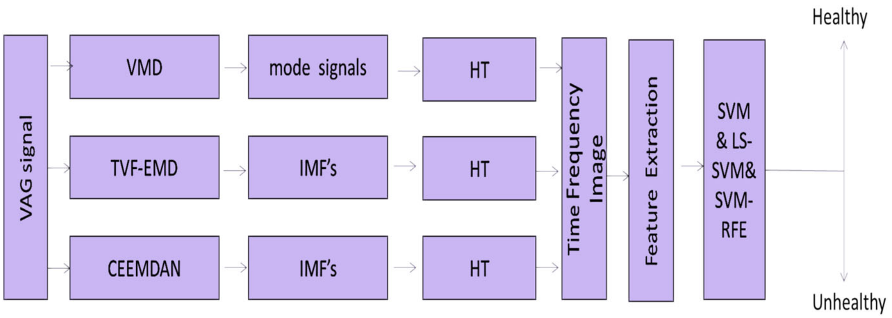

Fig. 1 Block diagram for VAG signal processing and feature analysis

that entails identifying local extrema, interpolating them to create an envelope, and then subtracting the mean of this envelope from the signal. This iterative sifting process continues until the remaining component no longer has any significant oscillatory content, effectively isolating one IMF at a time. The next step involves removing the extracted IMF from the signal, and the decomposition process is repeated on the residual signal to isolate the next IMF.

This process of sifting, envelope creation, and mean subtraction is repeated until the signal is completely decomposed into a finite set of IMFs, each representing a different frequency component of the original VAG signal, from the highest frequency down to the lowest. The added noise assists in achieving a more accurate decomposition, and ensemble averaging over several noise realizations is applied to reduce the residual noise influence in the final IMFs. The result is a series of IMFs that capture the signal's distinct oscillatory patterns across different time–frequency scales, which are particularly useful for analyzing the biomechanics of knee joint health in a data-driven manner. Figure 1 above explains the overall block diagram of the feature extraction methods. This is designed to work well for data that is non-stationary and nonlinear frequency images that will give input to the time–frequency image. The features extracted from time–frequency images were classified using SVM, LS-SVM, and SVM-RFE, which are machine-learning algorithms. Finally, the healthy and unhealthy categories are identified in Fig. 1.

2.1 Empirical Mode Decomposition (EMD)

EMD is an input data-dependent adaptive time–space analysis technique.it is relevant to the decomposition of nonlinear and non-stationary signals to symmetric ones; EMD performs the function of separating a series into modes (intrinsic mode function) without leaving time series. Amplitude and frequency modulated factor also it depends on signal, length and sum of oscillatory as Intrinsic Mode Functions (IMF's). IMFs of the signal are considered as the following two conditions are satisfied. One is the number of maxima or minima (extrema). The number of zero crossings must be equal or differ by one, and another one is upper and lower envelope (local mean) must be the mean is zero. EMD decomposes the signal into a number of intrinsic mode functions (IMFs). However, mode mixing is one of the most difficult aspects of EMD [7]. In mode mixing, a single IMF consists of signals having different scales. This may lead to serious aliasing effects in time–frequency distribution, and the resultant IMFs may lose their physical significance.

A single time series could be empirical EMD decomposed to a residual [26]. The main modes are named intrinsic mode functions (IMFs) and are represented as $e(t)$ as shown in Eq. (1) is a time series, $u_i(t)$ is IMFs from 1 to N, and the iteration residual is $r(t)$. Repetition processes and shifting can derive IMFs.

$$e(t) = \sum_{i=1}^{N} u_i(t) + r(t) \tag{1}$$

One of the properties of EMD is both model oscillations within their intrinsic scale bandwidth also detail for time-varying filter bank, including these within a single cycle as intra-wave modulations [23]. Figure 2 represents the Empirical Mode Decomposition EMD algorithm steps. EMD break a signal into its component IMFs. An IMF is a function which has only one extreme between zero crossings and a mean value of zero.

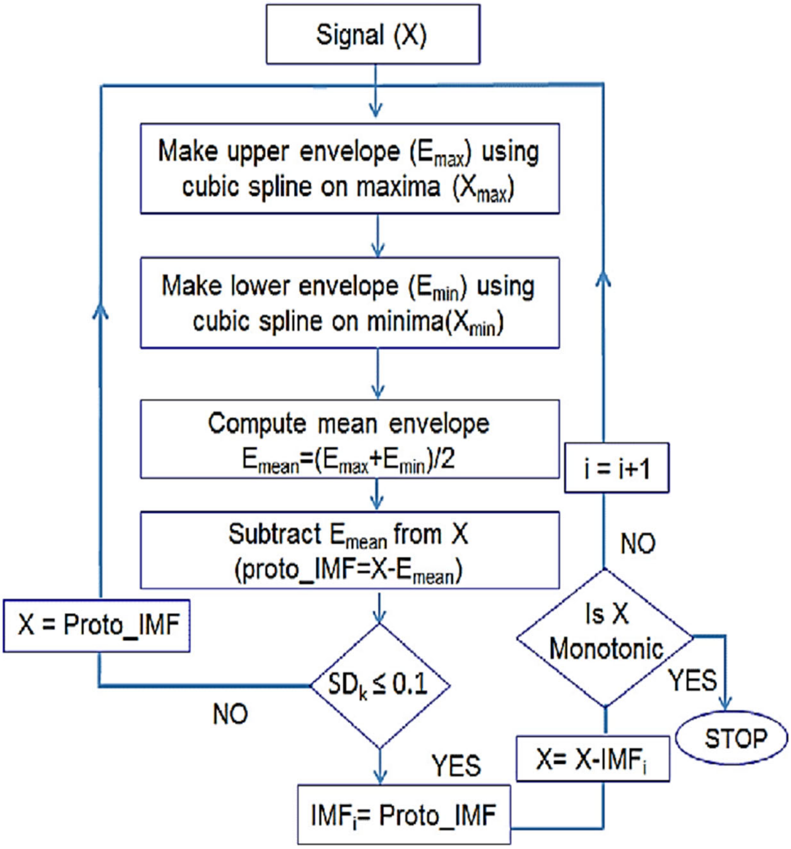

Fig. 2 Flowchart for empirical mode decomposition (EMD)

Once the IMFs are derived, the Sifting Process is enabled. The sifting process is what EMD uses to decompose the signal into IMFs [11]. Let a signal $X(t)$, for m_1 is the mean of its upper and lower envelopes as determined from a cubic spline interpolation of local maxima and minima. Proto_IMF denotes the mean value extracted from the combination of upper and lower envelope of the VAG signal.

An arbitrary parameter determines the locality; the computational time and the effectiveness of the EMD depend greatly on a parameter. The first component h_1 is calculated using Eq. (2).

$$h_1 = X(t) - m_1 \tag{2}$$

In the shifting process of the Empirical Mode Decomposition (EMD) method, upper and lower envelopes play a critical role in isolating the intrinsic oscillatory modes, or Intrinsic Mode Functions (IMFs), from a signal. These envelopes are constructed by identifying the local maxima and minima points within the signal and interpolating them, typically using cubic splines to form smooth boundary curves. The upper envelope connects all the local maxima, while the lower envelope connects all the local minima. The mean of these two envelopes is then calculated to capture the local trend of the signal at each point in time. In the second sifting process, h_1 is treated as the data, and m_1 is the mean of h_1 is upper and lower envelopes as of Eq. (3)

$$h_{11} = X(t) - m_{11} \tag{3}$$

The sifting process is repeated k times until h_1k is an IMF, that is:

$$h_1(k-1) - m_1k = h_1k \tag{4}$$

Then, it is designated as $C_1 = h_1k$, the first IMF component from the data, which contains the shortest period component of the signal, then separates it from the rest of the data: $X(t) - C_1 = r_1$. The process is repeated to r_1 as follows:

$$r_1 - c_2 = r_2, r_3, \ldots..r_{n-1} - c_n = r_n \tag{5}$$

This results in a set of mode functions; the number of functions in the set depends on the original signal.

2.2 Complete Ensemble Empirical Mode Decomposition with Adaptive Noise (CEEMDAN)

The CEEMDAN has a variation of the EEMD algorithm, and it provides an exact reconstruction of the original signal and a better spectral partition of IMFs. In CEEMDAN, using to decompose the VAG signal into IMFs. In the CEEMDAN model, the timestamps for segregating the signals were kept constant at 5 Seconds. EEMD successfully minimized the mode mixing problem. As a result of dissimilar, residual noise for the number of modes would be unequal. The CEEMDAN method reduces the computations of EEMD and ensures the definite recovery of the data. The modified version of Hilbert Huang Transform (HHT), known as CEEMDAN- HHT, and the traditional HHT combination of Empirical Mode Decomposition and Hilbert transform will be used [14].

Let E_k be the function to generate the kth mode or IMFs from the EMD method as represented as $E(s) = x - M(s)$ here s is the input signal and M (.) be a function that outputs the local mean of the input signal. The 1st mode, or IMF's E_1, is illustrated as follows

$$E_1(s) = s - M(s) \tag{6}$$

Thus by considering the various modes of the computed IMFs as an input, the CEEMDAN algorithm can be computed as shown in algorithm 1.

Algorithm 1 Complete ensemble empirical mode decomposition with adaptive noise

Input	Different modes of IMFs $E_1(s), E_2(s), E_3(s) \ldots . E_n(s)$
Output	Recovered mode functional data for feature computation
Begin	
Step 1:	for every white noise with zero mean $w(i)$ the positive constant is denoted as β_0 and in general term for $\beta_{k-1} > 0$ where k denotes the mode number
Step 2:	Calculate the set of ensembles as $S^i = S + \beta_0 E_1(W^i)$
Step 3:	The local of mean with 'I' realization is calculated by traditional EMD method M (.) for the set of ensembles to get the 1st residue as represented in the equation $r_1 = M(S^i)$ Where (.) performs the averaging function overall i ∈ (1,2 , . . . , I)
Step 4:	For the first mode $C_1 = S - r_1$
Step 5:	Calculate the second residue using $C_2 = r_1 - M(r_1 + \beta_1 E_2(W^i))$
Step 6:	Update the K value and generalize the residue as $r_k = M(r_{k-1} + \beta_{k-1} E_k(W^i))$
Step 7:	Calculate the Kth mode as $C_k = r_{k-1} - r_k$
Step 8:	Repeat steps 2 to 7 for the next mode until the residue r_k cannot be further decomposed by EMD.
Step 9:	Set the Constant as $\beta_k = \varepsilon_k . std(r_k)$
Step 10:	End if
Step 11:	End for
Step 12:	Return the recovered mode functional data
End	

The value of β has been set so that 0 is a reciprocal of SNR between the input signal and the added Gaussian white noise and in terms of standard deviation (SD) as given in Eq. (7).

$$\beta_0 = {}^{\varepsilon_0 * \sigma(s)}\Big/_{\sigma(E_1(W^i)} \tag{7}$$

There are two approaches for setting the stop-the-shifting criteria. First by a fixed number of shifting iterations and second based on energy parameters.

2.2.1 Hilbert Transforms

In order to achieve the analytical signal z (t), Hilbert transform is applied to the signals using the following Eq. (8).

$$\mathrm{z(t)} = \mathrm{s\ (t)} + \mathrm{j} * \mathrm{h\ (t)} \tag{8}$$

Here, s (t) input signal and h (t) Hilbert transform of the input signal, which is represented as follows

$$\mathrm{h(t)} = \frac{1}{\pi}\mathrm{P}\int_{-\infty}^{\infty}\frac{s(\tau)}{t-\tau}\mathrm{d}\tau \tag{9}$$

Cauchy principal value with singular integral represented as P.

2.3 Time-Varying Empirical Mode Decomposition (TVF-EMD)

A single time series of nonlinear and linear or non-stationary and stationary components could be decomposed by EMD [34]. Using the least square SVM method and avoiding the complexity of masking signals not being adaptively tested, as the masking signal may not always enable the EMD to generate true single component Intrinsic Mode Functions (IMFs). Thus, the established assisted signal is adaptive and relevant for the analysis of frequency-varying components. TVF-EMD will solve the traditional EMD if the traditional EMD fails to isolate the modes whose frequencies are time-varying and lie within an octave and fails to remove the time-varying frequency in mode mixing [3]. The sifting process is completed using the time-varying filter technique. The local cut-off frequency is flexible and designed to facilitate instantaneous amplitude and frequency information [19].

Next, non-uniform B-spline estimation is adopted with a time-varying filter, improving the performance under low sampling rates and a bandwidth criterion for intrinsic mode function (IMF) [33]. TVF-EMD is entirely adaptive and suitable for analyzing linear and non-stationary signals. Compared with EMD, the TVF-EMD method improves frequency separation performance and stability under low sampling rates [30]. Figure 3 represents the Time Varying Empirical Mode Decomposition (TVF-EMD) algorithm steps.

Step 1: Let's consider the X(t) is a continuous input signal.

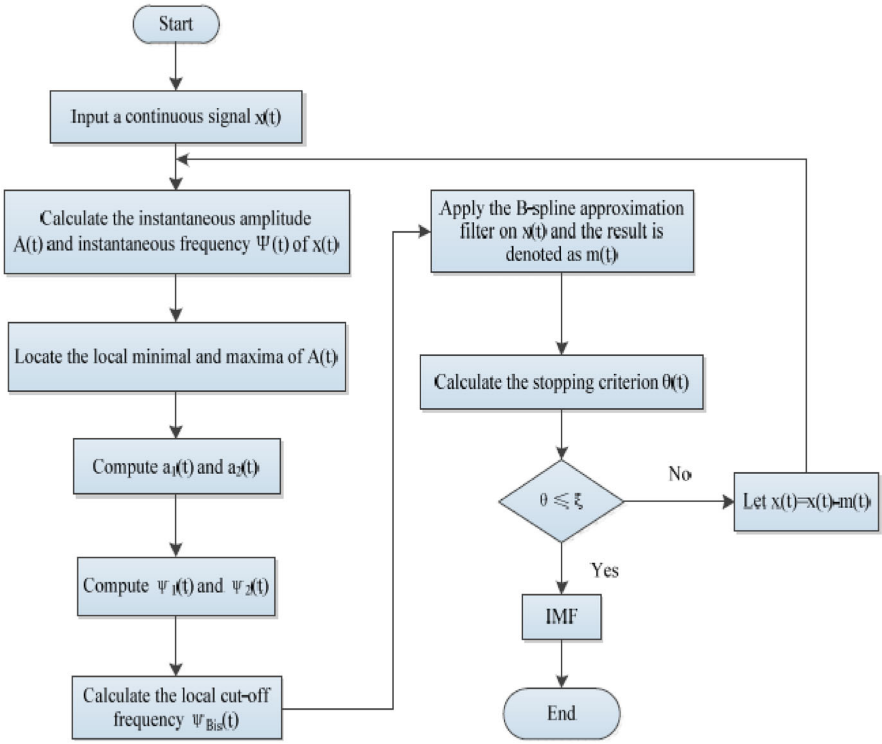

Fig. 3 Flowchart for time-varying frequency empirical mode decomposition (TVF-EMD)

Step 2: Calculate the instantaneous amplitude A(t) and instantaneous frequency ψ(t) of X(t) and locate the minima and maxima of A(t).

Step 3: Compute A_1(t) and A_2(t) and compute ψ_1(t) ψ_2(t) as well as calculate the local cut of frequency ψ_{Bis} (t).

Step 4: Applying the B-spline approximation filter on x(t), and the result is denoted by m(t) calculating the stopping criterion θ(t).

Step 5: Check $\theta \leq \xi$ If the condition is no, then perform let X(t) = X(t)-m(t), and if the condition is true, then it is processing IMF of decomposes the signal repeated this process when the condition is satisfied.

2.4 Variational Mode Decomposition (VMD)

VMD is an advanced method for disintegrating a multiple component into Band-Limited Intrinsic Mode Functions (BLIMFs) [31]. It decomposes the input signal into subsignals, which are represented as uk. VMD illustrates a stiff variational problem. Wk is the centre of pulsation, and the modes are dense around it. The number of BLIMFs, which is set to 5 in this case, provides more explanation.

$$\min_{\{uk\}.\{wk\}}\left\{\sum_{k=1}^{k}\delta_t\left[(\delta(t)+\frac{j}{\pi t})*u_k(t)]e^{-jw_k t}\frac{2}{2}\right.\right\} \tag{10}$$

Subject to $\sum_{k=1}^{k} u_k = \mathrm{f}$.

Variational Mode Decomposition is used to overcome empirical mode decomposition, such as sensitivity to noise samplings. The VMD model is examined as a total number of modes and their various centre frequencies because the modes reproduce the input signal while being smoother and then demodulation to the baseband [13]. The variational model decomposition is accurately optimized using a multiplier approach with different direction methods. The VMD method had good results when compared with other decomposition methods like the empirical mode decomposition (EMD) in the decay of actual and artificial data [24]. The VMD has been used in past works to denoise images.

The computational process of the VMD algorithm is as follows:

Algorithm 2 Variational mode decomposition

Input	Different modes of IMFs $E_1(s), E_2(s), E_3(s) \ldots . E_n(s)$
Output	Recovered mode functional data for feature computation
Begin	
Step 1:	Initialize$\{u_k^1\}\{\omega_k^1\}$,Λ^1 and n to zero.
Step 2:	n = n + 1, execute the entire loop
Step 3:	Execute the loop if k = k + 1 until k = K, update uk: u_k^{n+1}=argminL($\{u_{i<k}^{n+1}\}$,$\{u_{i\geq k}^n\}$,$\{u_i^n\}$,Λ^n)
Step 4:	Execute the loop for k = k + 1 until k = K, update ωk: ω_k^{n+1} = argminL($\{\omega_{i<k}^{n+1}\}$,$\{\omega_{i\geq k}^n\}$,$\{\omega_i^n\}$,Λn)
Step 5:	Use $\Lambda^{n+1} = \Lambda_n + \tau(f(t) - \sum_k u_k(t)$ to update Λ;
Step 6:	Given the discrimination condition $\varepsilon > 0$, when the iteration stop condition is satisfied, all the loops are stopped, and the result is output, and K IMFs are achieved.
Step 7:	End if
Step 8:	End for
Step 9:	Return the recovered mode functional data
End	

2.5 Classification Using Different SVM Algorithms

After the Hilbert transformation, the time–frequency image is produced. The features extracted from the time–frequency image are given input into LS-SVM (a classifier), and the performance is calculated.

2.5.1 Support Vector Machine (SVM)

Support Vector Machine is effective and mostly used for classification problems such as binary class classifications; maximal margin using separating hyperplanes between the positive and negative classes are constructed by SVM. It can handle a quadratic programming problem containing inequality constraints with a linear cost on the slack variables [25]. However, the dual space is solved, and it is better feasible. To choose the convenient kernels for the SVM, as compared the polynomial kernels, Gaussian kernels, and sigmoid kernels, and found that the polynomial kernels can help the SVM produce the best classification accuracy and confusion matrix results over the current dataset [21]. Thus, the SVM with quadratic kernels to process the knee joint VAG signal classification is expressed as.

1. Choose a kernel function,
2. Choose a value for C that has a regularization parameter,
3. Solve the quadratic problem programming as given in Eq. (11),

$$\sum_{i=1}^{n} \alpha_{\mathrm{j}} - \frac{1}{2}\sum_{i=1}^{n}\sum_{j=1}^{n} \alpha_{\mathrm{i}}\alpha_{\mathrm{j}}\mathrm{y_i y_j K(x_{i,}\, x_j)} \tag{11}$$

$$0 \le \alpha_{\mathrm{i}} \le \mathrm{C} \quad \sum_{i=1}^{n} \alpha_{\mathrm{i}}\mathrm{y_i} = 0$$

   The quadratic programming problem is represented in dual Lagrangian form, where C is a constant that bounds the misclassification error. Unlabelled instances are classified using the learned parameters αi and bias b.
4. Construct the discriminant function from the support vectors using the sign of the decision function as given in the following Eq. (12)

$$\mathrm{g(x)} = \sum_{i \in SV} \alpha_{\mathrm{i}}\mathrm{K(X_i,\, X) + b} \tag{12}$$

2.5.2 Least Square-Support Vector Machine (LS-SVM)

One of the supervised learning methods for LS-SVM is used for data analysis and pattern classification. LS-SVM is an upgraded version of a support vector machine. In LS-SVM, the result is achieved by solving linear equations instead of complex quadratic programming. The pixel intensity is used to calculate the feature measures

[22]. Each pixel corresponds to the distinct time and frequency that defines the power of the signal at any precedent of the frequency.

We are extracting statistical features such as mean, standard deviation, and inequality from all the pixel intensities corresponding to each time–frequency image. Thus, from these statistical values, we can obtain the analysis of the main information as attributes of the signal. The advantage of using the LS-SVM algorithm over the standard SVM is the learning efficiency of similar linear equations. The SVM algorithm for pattern recognition minimizes the quadratic problem and slack variable as well. The quadratic programming problem reduces a set of matrix inversion functions in the dual space, which takes less time compared to solving the SVM quadratic problem. The standard LS-SVM is the training of N pairs of data points {xk,yk}$k = 1N$, where xk ∈ , Rn,yk ∈ , {− 1,1} solve the LS-SVM is equivalent to determine the linear equations.

Algorithm 3 Least square support vector machine

Input	Training set S:={(xk, yk)} $_{k=1}^{N}$ and a learning rate 0< η <2N
Output	(β, b) define LS-SVM
Begin	
Step 1:	β ← 0, b← 0,scalar =1-$\frac{\eta}{n}$
Step 2:	repeat For k=1 to N e← y_k - $\sum_{j=1}^{N} \gamma\eta\beta_j\langle x j , xk\rangle$-b
Step 3:	for j=1 to N
Step 4:	if (j=k)β_j←scalar* β_j +e;
Step 5:	else βj←scalar* βj;
Step 6:	end for
Step 7:	b← $b + \gamma\eta e$;
Step 8:	until the convergence criterion is satisfied
Step 9:	return (β, b);
End	

2.5.3 SVM—Recursive Feature Elimination (SVM-RFE)

The SVM-RFE algorithm is an envelope feature selection method that generates the ranking of features using backward feature elimination. It was originally proposed to perform gene selection for knee joint classification. It's based on eliminating redundant genes and returning better and more compact gene subsets. The features are eliminated given to a criterion related to their support of the discrimination function, and the SVM is retrained at each step [10]. RFE-SVM is a weight-based algorithm at every step; the coefficients of the weight vector of a linear SVM are used as the feature ranking criterion. The RFE-SVM algorithm steps are shown in algorithm 4.

Algorithm 4 SVM—recursive feature elimination algorithm

Input	Initial input gene subset G= {1,2,..n}
Output	find out the smallest weight Set R ={}
Begin	
Step 1:	Train the SVM using G;
Step 2:	Compute the weight vector using the equation W= $\sum_{i=1}^{n} \beta_i x_i y_i$ Here, i is the number of genes ranging from 1 to n; β_i is the Lagrangian Multiplier estimated from the training set; x_i is the gene expression vector for sample i and y_i is the class label of i ($y_i \in [-1,+1]$)
Step 3:	Compute the Ranking Criteria Rank =W^2
Step 4:	Rank the feature as in sorted manner as New rank = sort (Rank)
Step 5:	Update the Feature Rank list as Update R=R+G(New rank)
Step 6:	Eliminate the feature with smallest rank Update G=G-G (New $_{rank}$)
Step 7:	Repeat steps 2 to 6 until G is non-Empty
Step 8:	End the output of Rank list according to the smallest weight criterion R.
Step 9:	Repeat the process with the training set restricted to the remaining features.
End	

Feature Sorted List New_{rank}. In each loop, the feature with minimum (w^2) will be removed. The SVM then retrains the remaining features to achieve the new feature sorting. SVM-RFE repeated the process until achieving a feature-sorted list. Through training SVM using the feature subsets of the sorted list and evaluating the subsets using the SVM prediction accuracy, we then achieve the optimum feature subsets.

3 Results and Discussion

3.1 Results for Variational Mode Decomposition (VMD)

The VAG signals are given an input to the VMD algorithm. The VAG signals have composite input values, and the input values are passed into the different frequency levels that are represented in Fig. 4.

The VAG signals are decomposed into the IMF's signal. The VMD signals to perform mode signal operation. The VMD method is used to examine the total number of modes and their centre frequencies, and the mode reproduces the input signals while being smooth and demodulating the baseband of spectral decomposition shown in Fig. 5.

Spectrum-based decomposition of the VAG signal into any band with a number of modes. The modes are extracted concurrently using a non-recursive variation mode decomposition model. The model is shown for an ensemble of modes, then their corresponding centre frequencies, such as the modes collected and reproduces the

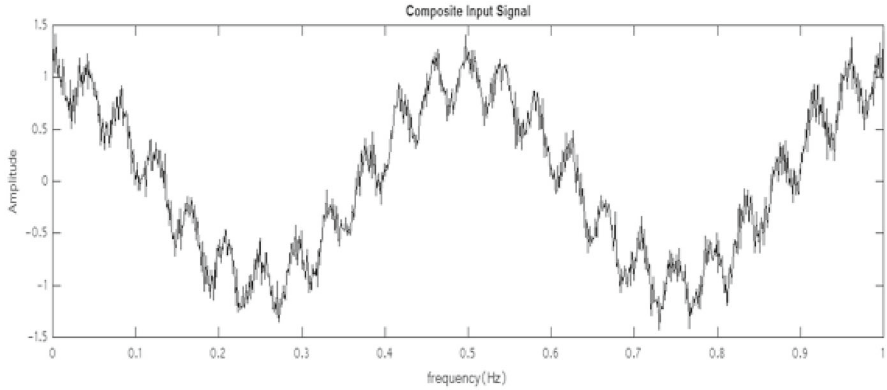

Fig. 4 Composite input signal for VMD method

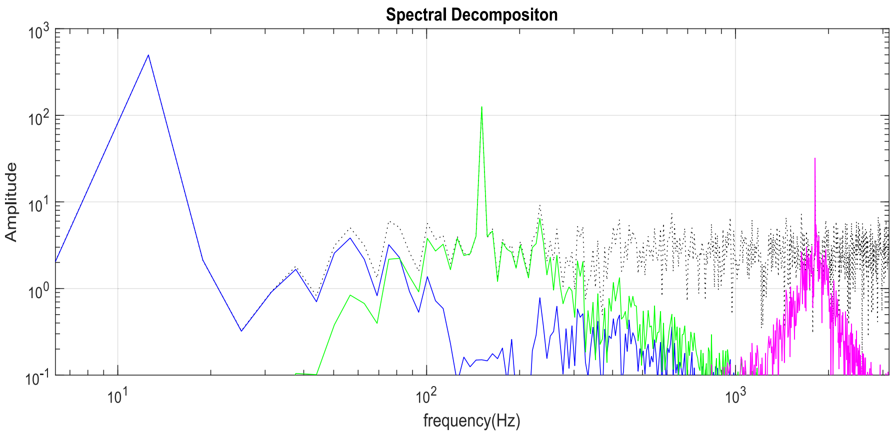

Fig. 5 Spectral decomposition for the VMD method

input signal of each being smooth after demodulation into baseband, as shown in Fig. 6.

3.2 Result for Time-Varying Frequency Empirical Mode Decomposition (TVF-EMD)

The sampling rate and rad frequency are used to analyze the signal and add the noise signal to linear and non-stationary VAG signals. Time-varying filtering-based EMD results in the intrinsic mode function using Hilbert transformation to extract the instance of amplitude and instance of frequency. Compute the basic cut-off frequency to deal with the mode mixing problem to locate the maxima of the input signal after Preprocessing found all the intermittences. When two or more successive points have the same value, we consider only one extremum in the middle of the constant area,

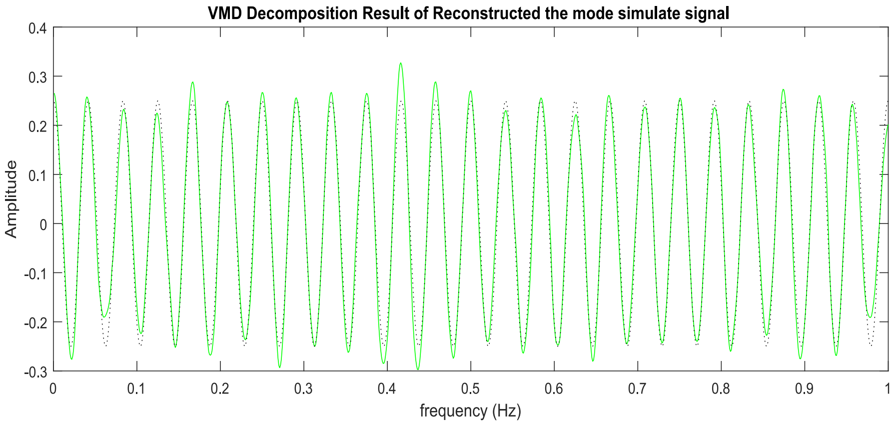

Fig. 6 Reconstructed mode of input signal for the VMD method

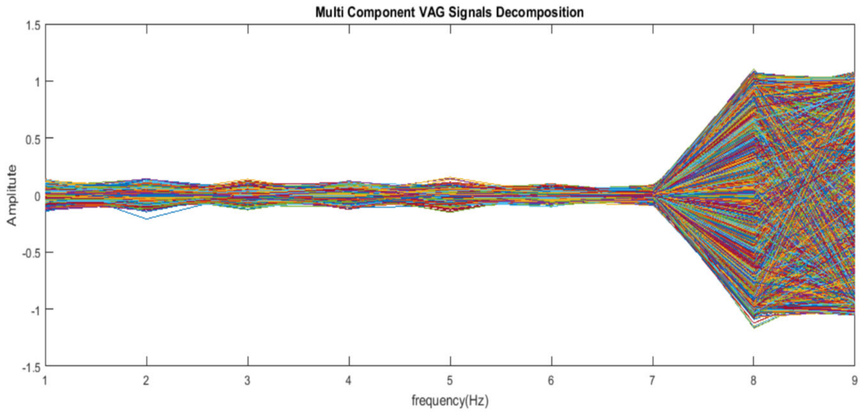

Fig. 7 Multi-component VAG signal was decomposition using TVF-EMD

and it is extracted using Gabriel Rilling. Multi-component VAG signal decomposition using TVF-EMD was shown in Fig. 7.

3.3 Result for Complete Ensemble Empirical Mode Decomposition with Adaptive Noise (CEEMDAN)

Consequent signals interfere with the mode mixing problem that occurs in EMD processing and generate exact aliasing in IMFs, and they may conceal the physical characteristics of each IMF in the time–frequency domain. IMF's = EMD(x) where X is a real vector that computes the Empirical mode decomposition, resulting in a matrix IMF containing 1 IMF per row, the last one being the residue. If the X is a complex vector, it computes the Bivariate Empirical mode decomposition of x, resulting in a matrix IMF containing 1 IMF per row, the last one being the residue. The default stopping criterion is the proposed one. It calculates the sampling time and maximum number of shifting iterations for the computation of each mode and also extracts the maximum number of IMFs. If it displays is equal to 2 shifting process steps without pause, then when the input is complex, the display is disabled. Masking signal used to improve the decomposition. When comparing Complete Ensemble Empirical Mode Decomposition with Adaptive Noise (CEEMDAN) and Variational Mode Decomposition (VMD) in result analysis, key differences emerge in terms of their decomposition approach, robustness to noise, and computational efficiency. CEEMDAN is a noise-assisted, adaptive method that iteratively decomposes a signal into Intrinsic Mode Functions (IMFs) by adding white noise to prevent mode mixing and improve the separation of frequency components. This noise-assisted approach yields highly adaptive decompositions, making CEEMDAN well-suited for non-linear, non-stationary signals like biomedical data, where it can accurately isolate intrinsic oscillatory modes. However, CEEMDAN can be computationally intensive, as it requires multiple noise realizations and iterative sifting to achieve stable IMFs, which may introduce computational delays in real-time applications. The decomposition phases using CEEMDAN is shown in Fig. 8.

The CEEMDAN results displayed in the image showcase a series of Intrinsic Mode Functions (IMFs) decomposed from an original input signal, which appears to be a non-linear and non-stationary biomedical signal, possibly an ECG or vibroarthrographic (VAG) signal based on the typical frequency patterns visible in the top panel. Each row in the plot represents an IMF, which has been iteratively extracted from the original signal through the CEEMDAN process. The top IMFs capture high-frequency oscillatory components, which are likely to correspond to fast-varying details or noise

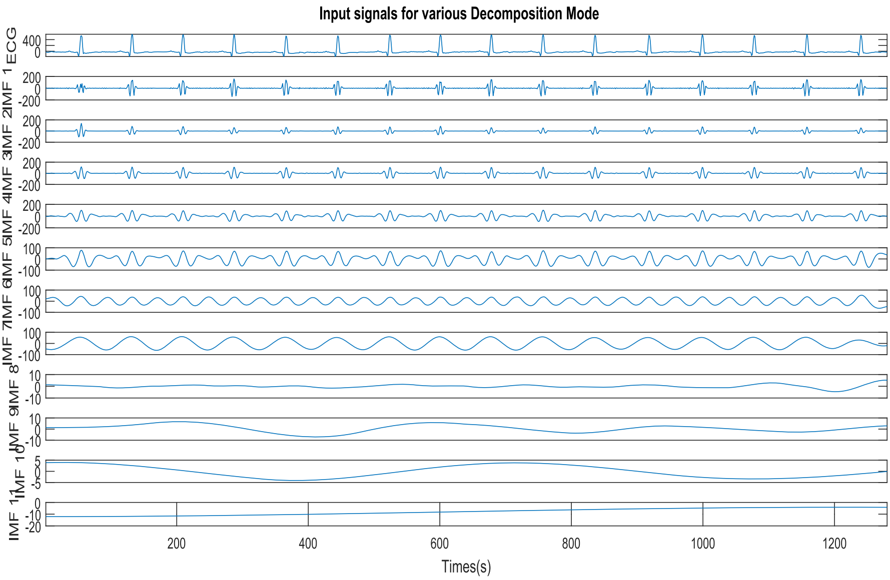

Fig. 8 Signal decomposition using the CEEMDAN model

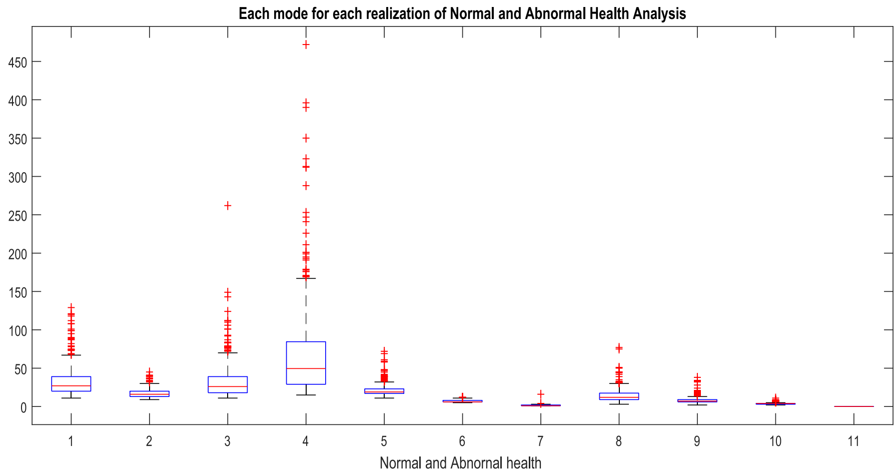

Fig. 9 Shifting iteration of each mode for each realization of normal and abnormal health

inherent in the input signal, while lower rows display IMFs that progressively represent slower, low-frequency components. The high-frequency IMFs show rapid oscillations with minimal amplitude, indicative of finer details in the signal, while the IMFs in the middle and lower parts exhibit smoother, more pronounced oscillations, representing the fundamental modes and the underlying trends in the data. As we move further down the rows, the IMFs tend to capture broader, slower-varying components that may represent baseline or trend-like patterns within the signal. The bottom-most component could potentially capture the residual or trend component, which represents the overall low-frequency baseline of the original signal. This decomposition allows for a detailed time–frequency analysis of the signal, separating noise, fine details, and underlying trends into distinct modes. This separation can aid in feature extraction and further analysis, such as identifying patterns associated with healthy versus unhealthy knee joints in VAG signals or detecting anomalies in ECG signals. Overall, the CEEMDAN results in this image provide a comprehensive decomposition that enables focused analysis of different frequency bands, enhancing interpretability and diagnostic accuracy. The scale partition capabilities of EEMD eliminate the problem of mode mixing. The CEEMDAN method improves the process of complete shifting in multiple-mode operation, as shown in Fig. 9.

3.4 Time–Frequency Image of Input Signal

In VAG signals of the waveform after decomposition, different frequencies of input signals of VMD, TVF-EMD, and CEEMDAN methods are given input to the time–frequency image which was shown in Fig. 10.

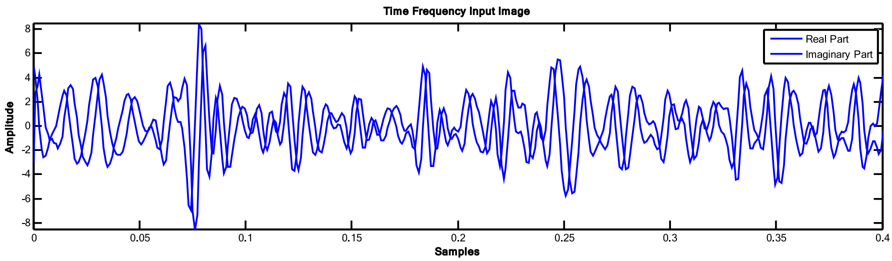

Fig. 10 Input signal of time–frequency image

3.5 Feature Extraction of Spectrogram Output

Time–frequency image is used for the feature detection method of scale invariant feature transformation for computer vision. The pixel intensity was used to measure and calculate the feature. Each and every pixel corresponds to a certain time and frequency that represents the power of the signal at any instance of frequency. Machine learning, using pattern recognition, measure the mean, standard deviation, skewness and kurtosis of all pixel intensity related to each time–frequency. It will detect the local features in the image as an oriented gradient, as shown in Fig. 11. Initially, we computed 18 features that have categories, including statistical, problem-related, time-domain, and frequency-domain features. After implementing the SVM-RFE model, the feature set was reduced to 11 features which have 4 statistical, 4 problem-related, 2 time-domain, and 1 frequency domain features with it. After feature detection, features are classified as the pattern of healthy and unhealthy signals using SVM and LS-SVM algorithms. To analyse and extract the healthy and unhealthy knee joint disorders, we have computed the sample folds, which are shown in Fig. 12.

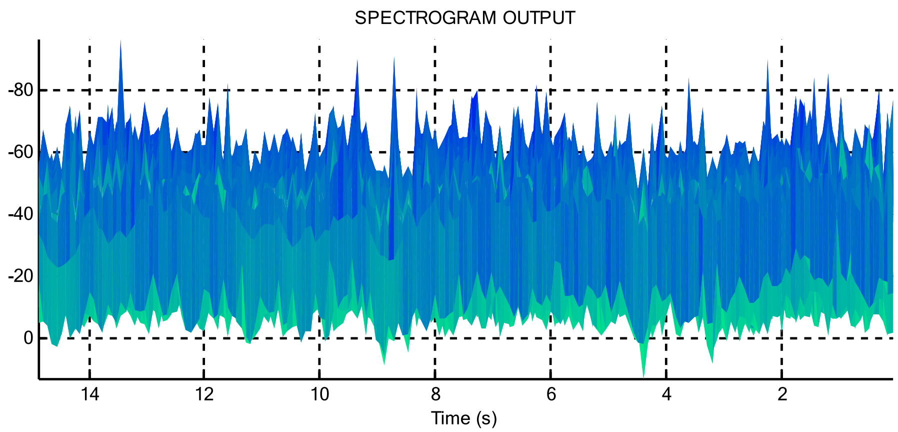

Fig. 11 Feature extraction of spectrogram output using LS-SVM

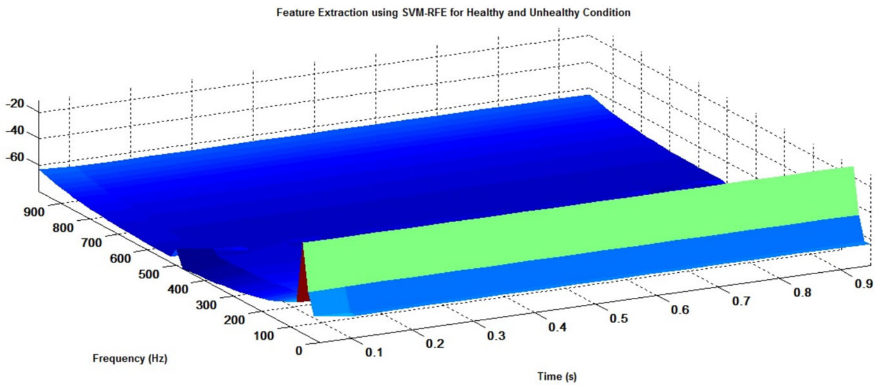

Fig. 12 Healthy and unhealthy samples fold using LS-SVM

4 Conclusion

The proposed system demonstrates a significant contribution toward low-power computing, particularly in biomedical signal analysis and real-time diagnostics. By leveraging techniques like TVF-EMD, VMD, and CEEMDAN to decompose VAG signals into intrinsic mode functions (IMFs) and perform Hilbert transformations, the system captures critical time–frequency features without extensive computational overhead. This is vital for low-power devices, as the adaptive nature of these decompositions inherently limits the need for high-frequency processing, reducing power consumption. The method also optimizes the shifting process to reconstruct input signals with noise resilience, a crucial feature for minimizing errors in noisy, real-world clinical environments. Using time–frequency images for LS-SVM and SVM-RFE classification offers a further power-efficient approach, as these algorithms, particularly SVM-RFE, maximize feature relevance while minimizing computation by selectively focusing on the most critical patterns. This enables the system to accurately classify healthy and unhealthy knee joints with minimal redundancy, crucial for embedded or portable healthcare devices that need efficient processing for continuous monitoring applications. Thus, the system's design addresses the dual challenges of accurate signal decomposition and power-efficient feature extraction, advancing the potential for scalable, low-power diagnostic tools in remote healthcare and wearable technology for joint disorder diagnosis.

Acknowledgements The authors extend their appreciation to the Deputyship for Research and Innovation, Ministry of Education, Saudi Arabia, for funding this research (IFKSUOR3-176-13).

Data Availability The dataset used for the findings will be shared by the corresponding author upon request.

Declarations

Conflict of interest The authors declare that they have no conflict of interest.

References

1. Ø. Bjelland, B. Rasheed, H.G. Schaathun, M.D. Pedersen, M. Steinert, A.I. Hellevik, R.T. Bye, Toward a digital twin for arthroscopic knee surgery: a systematic review. IEEE Access **10**, 45029–45052 (2022)
2. M.H. Chang, D.H. Kim, S.H. Kim, Y. Lee, S. Cho, H.S. Park, K.J. Cho, Anthropomorphic prosthetic hand inspired by efficient swing mechanics for sports activities. IEEE/ASME Trans. Mechatron. **27**(2), 1196–1207 (2021)
3. R. Chen, Y. Jiang, H. Ni, Optimal imaging time interval selection method for space target via time–frequency analysis with spaceborne ISAR. IEEE Geosci. Remote Sens. Lett. Sens. Lett. **20**, 1–5 (2023)
4. A.-C. Cocea, C.I. Stoica, Interactions and trends of interleukins, PAI-1, CRP, and TNF-α in inflammatory responses during the perioperative period of joint arthroplasty: implications for pain management—a narrative review. J. Pers. Med. **14**(5), 537 (2024)
5. P.-A. Deleu, A. Naaim, B.D. Bevernage, L. Chèze, R. Dumas, I. Birch, J.-L. Besse, T. Leemrijse, Changes in relative work of the lower extremity and distal foot joints after total ankle replacement: an exploratory study. IEEE Trans. Neural Syst. Rehabil. Eng. **31**, 4376–4381 (2023). https://doi.org/10.1109/TNSRE.2023.3328936
6. M. Guermoui, K. Gairaa, K. Ferkous, S. de Domingos, O. Santos Jr., T. Arrif, A. Belaid, Potential assessment of the TVF-EMD algorithm in forecasting hourly global solar radiation: review and case studies. J. Clean. Prod. **385**, 135680 (2023)
7. H.-P. Huang, S.-Y. Wei, H.-H. Chao, C.F. Hsu, L. Hsu, S. Chi, An investigation study on mode mixing separation in empirical mode decomposition. IEEE Access **7**, 100684–100691 (2019). https://doi.org/10.1109/ACCESS.2019.2930543
8. S. Jerban, E.Y. Chang, Du. Jiang, Magnetic resonance imaging (MRI) studies of knee joint under mechanical loading. Magn. Reson. Imaging **65**, 27–36 (2020)
9. Y. Khalifa, A.S. Mahoney, E. Lucatorto, J.L. Coyle, E. Sejdić, Non-Invasive sensor-based estimation of anterior-posterior upper esophageal sphincter opening maximal distension. IEEE J. Transl. Eng. Health Med. **11**, 182–190 (2023)
10. H. Li, Y. Cui, J. Wang, W. Zhang, Y. Chen, J. Zhao, Identification and validation of biomarkers related to lipid metabolism in osteoarthritis based on machine learning algorithms. Lipids Health Dis. (2024). https://doi.org/10.1186/s12944-024-02073-5
11. F. Liu, X. Zhao, Z. Zhu, Z. Zhai, Y. Liu, Dual-microphone active noise cancellation paved with doppler assimilation for TADS. Mech. Syst. Signal Process. **184**, 109727 (2023). https://doi.org/10.1016/j.ymssp.2022.109727
12. Z. Li, B. Shi, Research of fault diagnosis based on sensitive intrinsic mode function selection of EEMD and adaptive stochastic resonance. Shock. Vib. **2016**, 1–12 (2016). https://doi.org/10.1155/2016/2841249
13. L. Miaofen, L. Youmin, W. Tianyang, C. Fulei, P. Zhike, Adaptive synchronous demodulation transform with application to analyzing multicomponent signals for machinery fault diagnostics. Mech. Syst. Signal Process. **191**, 110208 (2023). https://doi.org/10.1016/j.ymssp.2023.110208
14. A.A. Mousavi, C. Zhang, S.F. Masri, G. Gholipour, Structural damage localization and quantification based on a CEEMDAN Hilbert transform neural network approach: a model steel truss bridge case study. Sensors **20**(5), 1271 (2020)
15. M.-G. Murariu, F.-R. Dorobanțu, D. Tărniceriu, A novel automated empirical mode decomposition (EMD) based method and spectral feature extraction for epilepsy EEG signals classification. Electronics **12**(9), 1958 (2023). https://doi.org/10.3390/electronics12091958

16. R. Murugan, A. Balajee, L. Senbagamalar, S.M. Ganie, 11 machine learning and signal processing methodologies to diagnose human knee joint disorders. Artif. Intell. Knowl. Process. Improv. Decis. Mak. Predict. **119** (2023)
17. G. Rajalakshmi, C. Vinothkumar, A. Anne Frank Joe, T. Thaj Mary Delsy, Vibroarthographic signal analysis of bone disorders using arduino and piezoelectric sensors. In: 2019 International Conference on Communication and Signal Processing (ICCSP), pp. 0082–0086. IEEE (2019)
18. R.M. Rangayyan, Y.F. Wu, Screening of knee-joint vibroarthrographic signals using statistical parameters and radial basis functions. Med. Biol. Eng. Comput. **46**, 223 (2008)
19. R. Satheesh, S. Rajan, Assessment of mode shape in power system using TVF-EMD and spectral analysis. Electr. Power Componen. Syst. **50**(6–7), 349–358 (2022)
20. M.S. Begum, A.V.M.B. Aruna, A. Balajee, R. Murugan, An artificial intelligent methodology to classify knee joint disorder using machine learning and image processing techniques. Cogn. Anal. Reinf. Learn. Theor. Tech. Appl. 167–187 (2024)
21. S. Sridevi, B. Indira, S. S. Dutta, S. Sandeep, A. Sreenivasan, Quantum enhanced support vector machine with instantaneous quantum polynomial encoding for improved cyclone classification. In: 2023 6th International Conference on Recent Trends in Advance Computing (ICRTAC), pp. 748–752. IEEE (2023)
22. Y. Sun, Z. Peng, J. Hu, B.K. Ghosh, Event-triggered critic learning impedance control of lower limb exoskeleton robots in interactive environments. Neurocomputing **564**, 126963 (2024). https://doi.org/10.1016/j.neucom.2023.126963
23. G. Tu, X. Dong, S. Chen, B. Zhao, Hu. Lan, Z. Peng, Iterative nonlinear chirp mode decomposition: a Hilbert-Huang transform-like method in capturing intra-wave modulations of nonlinear responses. J. Sound Vib. **485**, 115571 (2020)
24. P. Tu, J. Li, H. Wang, Y. Li, W. Xiang, A novel lower-limb coordination assessment scheme using multi-scale nonlinear coupling characteristics with sEMG. IEEE Trans. Instrum. Meas. **72**, 1–11 (2023)
25. M. Umar, Z. Sabir, M.A.Z. Raja, H.M. Baskonus, M.R. Ali, N.A. Shah, Heuristic computing with sequential quadratic programming for solving a nonlinear hepatitis B virus model. Math. Comput. Simul **212**, 234–248 (2023). https://doi.org/10.1016/j.matcom.2023.04.034
26. J. Wang, Du. Guifu, Z. Zhu, C. Shen, Q. He, Fault diagnosis of rotating machines based on the EMD manifold. Mech. Syst. Signal Process. **135**, 106443 (2020)
27. Y. Wang, F. Liu, Z. Jiang, S. He, Q. Mo, Complex variational mode decomposition for signal processing applications. Mech. Syst. Signal Process. **86**, 75–85 (2017)
28. Y. Wu, *Knee joint vibroarthrographic signal processing and analysis* (Springer, Berlin/Heidelberg, Germany, 2015)
29. C. Yang, Y. Tashiro, A. Lynch, Fu. Freddie, W. Anderst, Kinematics and arthrokinematics in the chronic ACL-deficient knee are altered even in the absence of instability symptoms. Knee Surg. Sports Traumatol. Arthrosc. **26**, 1406–1413 (2018)
30. Yu. Miaomiao, H. Yuan, K. Li, L. Deng, Noise cancellation method based on TVF-EMD with bayesian parameter optimization. Algorithms **16**(6), 296 (2023). https://doi.org/10.3390/a16060296
31. H. Zhang, Lu. Wenhuan, J. Wei, X. Huang, X. Yang, Lu. Xugang, Efficient singular spectrum mode ensemble for extracting wide-band components in overlapping spectral environments. IEEE Trans. Signal Process. **72**, 4666–4681 (2024). https://doi.org/10.1109/TSP.2024.3437450
32. L. Zhao, Z. Li, J. Zhang, B. Teng, An integrated complete ensemble empirical mode decomposition with adaptive noise to optimize LSTM for significant wave height forecasting. J. Mar. Sci. Eng. **11**(2), 435 (2023)
33. Y. Zhao, M. Zhang, Q. Ni, X. Wang, Adaptive nonparametric density estimation with b-spline bases. Mathematics **11**(2), 291 (2023)
34. J. Zheng, H. Pan, Mean-optimized mode decomposition: an improved EMD approach for non-stationary signal processing. ISA Trans. **106**, 392–401 (2020)

Authors and Affiliations

Surbhi Bhatia Khan[1,2,3] · A. Balajee[4] · S. Sheik Mohideen Shah[5] · T. R. Mahesh[4] · Mohammad Alojail[6] · Indrajeet Gupta[7]

✉ Surbhi Bhatia Khan
surbhibhatia1988@yahoo.com

A. Balajee
balajee.a@jainuniversity.ac.in

S. Sheik Mohideen Shah
Sheikme2005@src.sastra.edu

T. R. Mahesh
Trmahesh.1978@gmail.com

Mohammad Alojail
malojail@ksu.edu.sa

Indrajeet Gupta
indrajeet.gupta@sru.edu.in

1 School of Science, Engineering and Environment, University of Salford, Salford, UK

2 University Centre for Research and Development, Chandigarh University, Mohali, Punjab, India

3 Centre for Research Impact and Outcome, Chitkara University Institute of Engineering and Technology, Chitkara University, Rajpura, Punjab 140401, India

4 Department of Computer Science & Engineering, Faculty of Engineering and Technology, JAIN (Deemed-to-Be University), Bengaluru 562112, India

5 Department of Computer Science and Engineering, Srinivasa Ramanujan Centre, Sastra Deemed to be University, Kumbakonam, India

6 Management Information System Department, College of Business Administration, King Saud University, Riyadh, Saudi Arabia

7 School of Computer Science & AI, SR University, Warangal, Telangana 506371, India